TISSUE ENGINEERING: Part A
Volume 15, Number 12, 2009

DOI: 10.1089/ten.tea.2008.0653

Tissue Formation and Vascularization in Anatomically Shaped Human Joint Condyle Ectopically *in Vivo*

Chang H. Lee, M.S.,[1] Nicholas W. Marion, Ph.D.,[1] Scott Hollister, Ph.D.,[2] and Jeremy J. Mao, D.D.S., Ph.D.[1]

Scale-up of bioengineered grafts toward clinical applications is a challenge in regenerative medicine. Here, we report tissue formation and vascularization of anatomically shaped human tibial condyles ectopically with a dimension of $20\times15\times15\,mm^3$. A composite of poly-ε-caprolactone and hydroxyapatite was fabricated using layer deposition of three-dimensional interlaid strands with interconnecting microchannels (400 μm) and seeded with human bone marrow stem cells (hMSCs) with or without osteogenic differentiation. An overlaying layer (1 mm deep) of poly(ethylene glycol)-based hydrogel encapsulating hMSCs or hMSC-derived chondrocytes was molded into anatomic shape and anchored into microchannels by gel infusion. After 6 weeks of subcutaneous implantation in athymic rats, hMSCs generated not only significantly more blood vessels, but also significantly larger-diameter vessels than hMSC-derived osteoblasts, although hMSC-derived osteoblasts yielded mineralized tissue in microchannels. Chondrocytes in safranin-O-positive glycosaminoglycan matrix were present in the cartilage layer seeded with hMSC-derived chondrogenic cells, although significantly more cells were present in the cartilage layer seeded with hMSCs than hMSC-derived chondrocytes. Together, MSCs elaborate substantially more angiogenesis, whereas their progenies yield corresponding differentiated tissue phenotypes. Scale up is probable by incorporating a combination of stem cells and their progenies in repeating modules of internal microchannels.

Introduction

The treatment of articular cartilage lesions, including those in osteoarthritis, is a major health care burden.[1] A synovial joint condyle is the bone's articulating portion and consists of articular cartilage that integrates with well-organized subchondral bone. Articular cartilage consists of chondrocytes embedded in a hydrated extracellular matrix. Chondrocytes, despite their indispensable role in chondrogenesis and cartilage homeostasis, account for approximately 5% of the total cartilage volume in adults.[2,3] Chondrocytes receive nutrients by diffusion exchange with perichondrium, synovial fluid, and subchondral bone, because articular cartilage is devoid of vascular supply.[3,4] These structural characteristics of articular cartilage have ramifications in cartilage tissue engineering. First, mature cartilage has few progenitor cells, which are critical for regeneration.[3,5–7] Second, the importance of biocompatible polymers in cartilage regeneration is evident because approximately 95% of the adult cartilage volume is extracellular matrix.[2,3] Hydrogels are hydrophilic polymers capable of absorbing biological fluids and provide chondrocytes and/or progenitor cells with a scaffold that simulates the cartilaginous extracellular matrix.[8–11] Some of the many critical differences between articular cartilage and subchondral bone in the context of cartilage regeneration are the obligatory role of vascularization in bioengineered bone and the absence of vasculature in articular cartilage.

Current therapies for late-stage osteoarthritis are primarily total joint arthroplasty using synthetic prostheses of metal, plastics, and ceramics. Limitations of current prostheses include infection, wear debris, aseptic loosening, dislocation, and limited life span. The fundamental drawback of synthetic prostheses is their failure to remodel with native tissue.[12] Existing biologically based therapies, including autologous chondrocyte transfer and mosaicplasty, are designed for localized cartilage lesions rather than as a substitute for synthetic prostheses that replace the entire synovial joint condyle, and incomplete integration, suboptimal conformity of cartilage surface, altered cartilage phenotype, and donor site morbidity limit existing biologically based therapies.[13–16] No biologically based therapies exist for functional replacement of the entire synovial joint condyle.

We and others have reported the tissue engineering of the entire synovial joint condyle ectopically using cells and bioscaffolds.[8,15,17–21] Stratified layers of cartilage and bone structures with dimensions of the human temporomandibular joint condyles or phalangeal condyles have been formed

[1]Tissue Engineering and Regenerative Medicine Laboratory, Columbia University Medical Center, New York, New York.
[2]Scaffold Tissue Engineering Group, Department of Biomedical Engineering, University of Michigan, Ann Arbor, Michigan.

ectopically *in vivo* from several cell sources, such as a single population of bone marrow-derived mesenchymal stem cells (MSCs),[8,15,17–19,21,22] or differentiated chondrocytes and osteoblasts.[21,23] Previously bioengineered joint grafts have been limited to dimensions up to 5 to 11 mm in diameter and 3 to 7 mm in height.[8,17,18,21,23] A commercially available scaffold (20×20×5 mm) was seeded with auricular chondrocytes and implanted under a vascular skin flap *in vivo*.[24] However, cell survival may have been primarily dependent upon the smallest Z dimension of 5 mm and the vascular-rich environment.[24] Furthermore, a microscale three-dimensional (3D) weaving technique yielded anisotropic 3D woven structures that were infused with a chondrocyte–hydrogel mixture *in vitro*.[25] There is continuing interest in cartilage and joint regeneration using innovative approaches, but the dimensions of all *in vivo*–implanted scaffolds thus far reported are sufficient only for small joints such as the phalanges and the temporomandibular joint but not for large joints such as the human knee and hip joints. Scale-up is a critical roadblock in the translation of bioengineered grafts toward clinical applications but is inevitably associated with challenges of cell survival as well as diffusion of nutrients and metabolic products. Vascularization is required for nutrient diffusion and waste removal in regenerating tissue over a volume of 200 to 400 μm.[26,27] Therefore, the objective of the present study is to determine tissue formation and vascularization of anatomically shaped human tibial condyle scaffolds seeded with human MSCs (hMSCs) or their chondrogenic and osteogenic progenies ectopically *in vivo*. Accordingly, we seeded human MSCs or their osteogenic progenies in layer-by-layer fabricated scaffolds with 400-μm interlaid strands and microchannels of a composite of poly-ε-caprolactone (PCL) and hydroxyapatite (HA). Poly(ethylene glycol)-diacrylate (PEGDA) hydrogel (1 mm deep) encapsulating hMSCs or hMSC-derived chondrogenic cells was molded anatomically as an articular cartilage layer and infused into microchannels of the PCL–HA scaffold. The scaffold dimensions of 20×15×15 mm^3 approximately doubled those in previous work[8,17,18,21,23] and represent 25% of the anatomic size of the human proximal tibial condyle, which is also the maximum allowable implantation size in the dorsum of athymic rats. After 6 weeks of subcutaneous implantation, we discovered that MSCs elaborated substantially more angiogenesis, whereas MSC progenies yielded corresponding differentiated tissue phenotypes. These findings have implications in synovial joint regeneration in large animal models and patients who suffer from arthritis.

Materials and Methods

Fabrication of anatomically shaped human tibial condyle scaffold

The anatomical contour of a native cadaver adult human proximal tibial joint condyle (Fig. 1A) was acquired from computed tomography scans and manipulated using computer-aided design software (Rhinoceros, McNeel, Seattle, WA) for 3D reconstruction (Fig. 1B). A scaffold was designed to include the entire articular surface of the proximal tibial

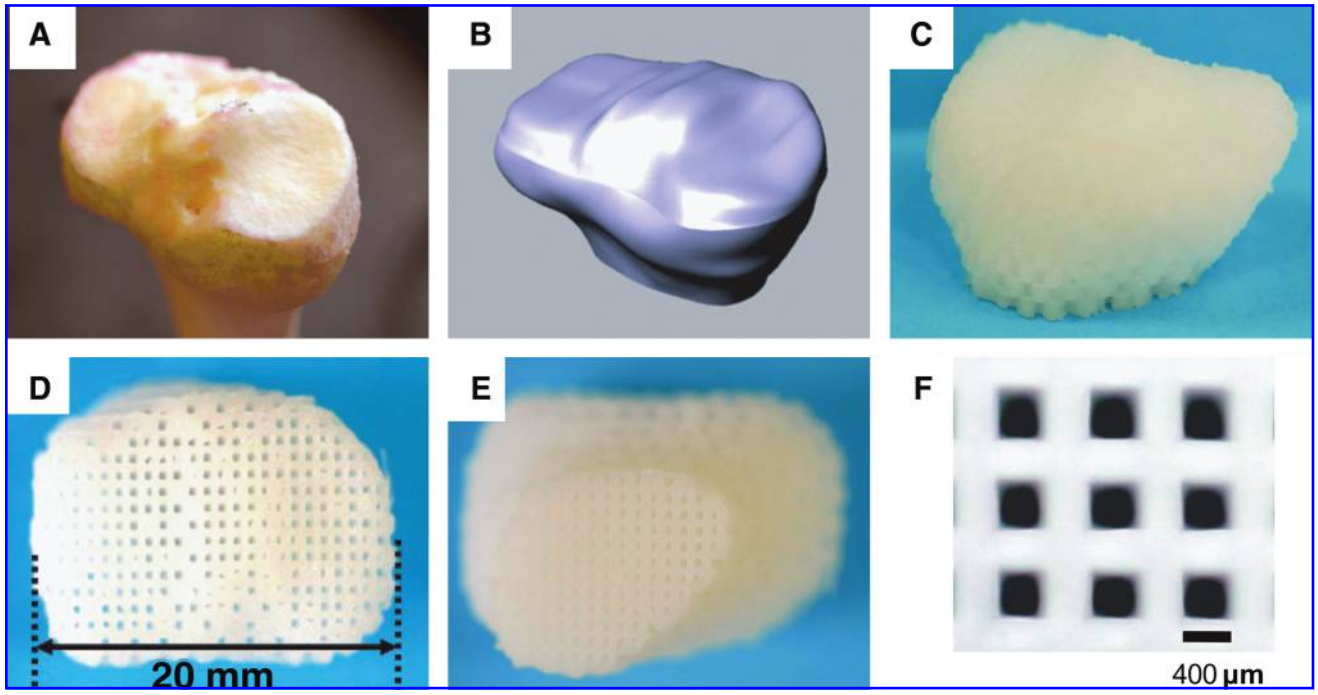

FIG. 1. Bioengineering design of the human-shaped synovial joint condyle. The anatomical contour of a cadaver adult human proximal tibial condyle showing medial and lateral articular surfaces (**A**) was captured using computed tomography scanning and manipulated using computer-aided design for three-dimensional (3D) reconstruction (**B**). A composite of poly-ε-caprolactone (PCL) and hydroxyapatite (HA) was co-melted into slurry and fabricated into anatomical shape and dimensions using layer deposition of 3D interlaid strands with repeating microchannels (400 μm) of the scaffold (**C–E**: sagittal, proximal, and distal views of the fabricated scaffold, respectively). The diameter of strands and inter-strand microchannels is 400 μm (**F**). Color images available online at www.liebertonline.com/ten.

condyle and subchondral bone in the dimension of $20\times15\times15\,mm^3$ (Fig. 1B), which equates to approximately 25% of the anatomic size of the human proximal condyle and represents the maximum implant size allowable in the dorsum of athymic rats. Engineering parameters were used to fabricate a composite polymer scaffold (Fig. 1C–E) using layer-by-layer deposition with a 3D printing system (Bioplotter, EnvisionTec, Berlin, Germany). The composite consisted of 80 wt% PCL (molecular weight (M_w) ~65,000, Sigma, St. Louis, MO) and 20 wt% of HA (Sigma, St. Louis, MO). PCL–HA was molten in the chamber at 120°C and dispensed through a 27-gauge metal needle (DL Technology, Haverhill, MA) to create interlaid strands and interconnected microchannels (diameter 400 μm) (Fig. 1F). The scaffold was sterilized in ethylene oxide for 24 h before cell seeding and *in vivo* implantation.

Seeding of hMSCs and hMSC-derived osteoblasts in scaffolds' microchannels

hMSCs were isolated from fresh bone marrow samples of multiple anonymous adult donors (AllCells, Berkeley, CA) per our prior methods.[17,28] Purification of hMSCs was accomplished by centrifugation through a density gradient (StemCell Technologies, Vancouver, Canada) and by negative selection following the manufacturer's protocol to remove hematopoietic and differentiated cells. Previously, we had further purified similarly isolated hMSCs and differentiated them into osteoblasts, chondrocytes, and adipocytes.[17,28] Culture-expanded second- or third-passage hMSCs were seeded at a density of 1×10^6 cells/mL in the microchannels of PCL–HA scaffolds (Fig. 2A). Cell suspension was repeatedly pipetted into the microchannels for 30 min, followed by 4 h of *in vitro* incubation to allow cell adhesion. Although this cell density may be considered somewhat low for bone regeneration, it is anticipated that a combination of the seeded human cells and migrated or recruited host-derived cells will contribute to tissue genesis.[19] A subset of PCL–HA scaffolds were seeded with hMSCs in the scaffolds' microchannels (Fig. 2B) and subsequently cultured for 4 weeks in 6-well plates with osteogenic-supplemented medium including 100 nM dexamethasone, 10 mM β-glycerophosphate, and 0.05 mM ascorbic acid-2-phosphate (Sigma), until a cartilage-intended portion was layered.

Hydrogel encapsulation of hMSCs and hMSC-derived chondrogenic cells

PEGDA (M_w 3400; Nektar, Huntsville, AL) was dissolved in phosphate buffered saline (6.6% w/v) supplemented with 133 U/mL of penicillin and 133 mg/mL of streptomycin (Invitrogen, Carlsbad, CA), and a photoinitiator (2-hydroxy-1-[4-(hydroxyethoxy) phenyl]-2-methyl-1-propanone; 50 mg/mL; Ciba, Tarrytown, NY). PEGDA solution suspended with hMSCs or hMSC-derived chondrogenic cells was photopolymerized with a long-wavelength (365 nm) ultraviolet light for 5 min (Glos-Mark, Upper Saddle River, NJ) in an anatomically shaped mold of the proximal human tibial condyle with a predefined 1-mm thickness (Fig. 2C) for immersing the scaffold to allow 1-mm hydrogel depth (Fig. 2D) and infused into the scaffolds' microchannels. For chondrogenic differentiation, culture-expanded second- or third-passage hMSCs were treated in medium supplemented with 10 ng/mL of transforming growth factor beta 3 (R&D, Minneapolis, MN), 1% insulin-transferrin-selenium, 1% antibiotics, 100 μg/mL of sodium pyruvate, 50 μg/mL of ascorbate, 40 μg/mL of L-proline, and 100 nM dexamethasone (Sigma). hMSCs or hMSC-derived chondrogenic cells at a density of 20×10^6 cells/mL were separately encapsulated in PEGDA hydrogel. This cell density was anticipated to be higher than that in adult articular cartilage in the range of 5% to 10% of tissue volume but was probably necessary in the early phase of cartilage regeneration.[21,23]

In vivo *implantation of bioengineered osteochondral construct*

Following Institutional Animal Care and Use Committee approval by the Columbia University Medical Center, 10-week-old athymic rats (Harlan, Indianapolis, IN) were anesthetized with 1% to 5% isoflurane. Upon disinfection with 10% povidone iodine and 70% ethanol, a 50-mm linear incision was made in the dorsum's midsagittal plane. After creation of subcutaneous pouches, the human-shaped proximal tibial condyle scaffold was implanted, followed by wound closure. One construct was implanted per rat because the construct at a dimension of $20\times15\times15\,mm^3$ is the maximum allowable implant size in the dorsum. Cell-free scaffolds were implanted as controls. After 6 weeks of *in vivo* implantation, all constructs were harvested upon carbon dioxide inhalation of host rats.

Histomorphometric and immunohistochemical analyses of in vivo *bioengineered human synovial condyle graft*

The harvested tibial condyle samples were embedded in polymethyl-methacrylate and sectioned sagittally at 5 μm thickness (HSRL, Jackson, VA). Randomly selected sections were stained with hematoxylin and eosin, safranin O, and von Kossa. Blood vessel numbers and diameters, cell numbers per unit area, and mineralized tissue volume over total tissue volume were quantified (Leica, Bannokburn, IL) per our prior methods.[8,29] Immunohistochemistry for type II collagen (ab3092) and osteopontin (ab69498) was performed per our prior methods.[8,29]

Data analysis and statistics

Upon confirmation of normal data distribution, all quantitative data of control and treated groups were treated using one-way analysis of variance and *post-hoc* least significant difference tests at an α level of 0.05 ($n = 10$ per group).

Results

Tissue formation and vascularization of in vivo *harvested bioengineered tibial condyle grafts*

hMSCs seeded in the scaffolds' microchannels (Fig. 2A) and cultivated *in vitro* for 4 weeks in osteogenic stimulating medium (Fig. 2B) attached to the microchannel wall. Upon seeding of hMSCs or hMSC-derived chondrogenic cells in the PEGDA hydrogel layer (Fig. 2C, D) that was infused into the scaffolds' microchannels, the entire osteochondral graft was implanted subcutaneously in the dorsum of athymic

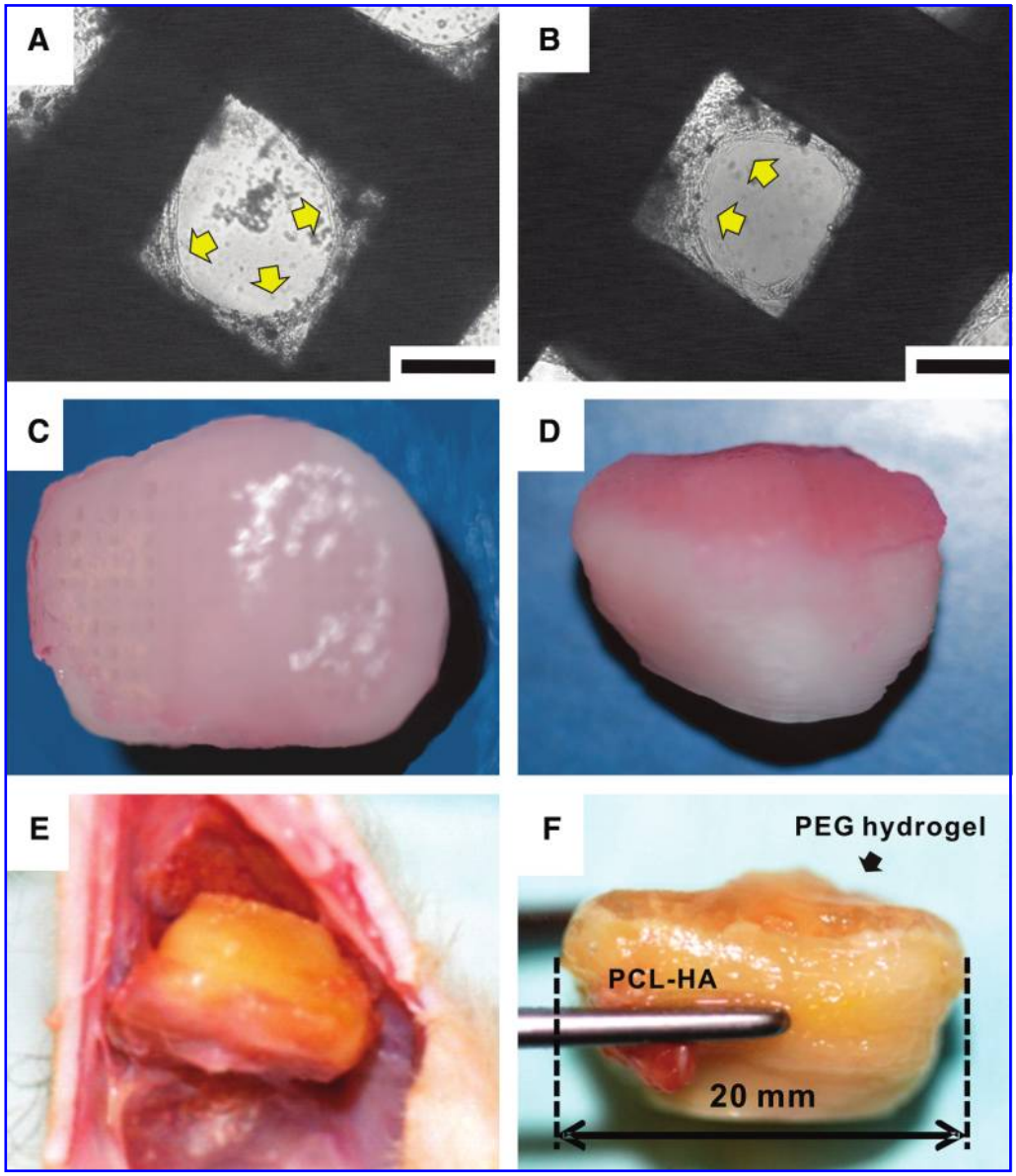

FIG. 2. Cell seeding and retrieval of *in vivo* implanted synovial joint condyle graft. Human mesenchymal stem cells (hMSCs) seeded in the scaffolds' microchannels (c.f. Fig. 1D) are attached to the surface of the microchannel wall after 4 weeks of culture *in vitro* (**A**). Similarly, hMSCs seeded in the scaffolds' microchannels and treated with osteogenic supplemented medium for 4 weeks *in vitro* are also attached to the microchannel wall (**B**). Arrows in **A** and **B** indicate cell attachment. Poly(ethylene glycol)-based hydrogel (PEGDA) (1 mm deep) encapsulating hMSCs or hMSC-derived chondrocytes, both at a density of 20×10^6/mL, was molded into the anatomic shape of the articular surface over the PCL–HA scaffold and was infused into microchannels (**C,** and **D** in superior and sagittal view). Upon retrieval 6 weeks postoperatively (**E**), the bioengineered tibial synovial joint condyle implant was integrated into host tissue and maintained the original shape (**F**). The bioengineered cartilage layer and bone layer can be readily distinguished and yet were integrated (**F**). Scale for **A** and **B:** 200 μm. Color images available online at www.liebertonline.com/ten.

rats. Harvested 6 weeks postoperatively (Fig. 2E), hydrogel and PLC–HA portions of the osteochondral scaffold were integrated to host tissue and maintained the original shape of the human proximal tibial condyle (Fig. 2F). No delamination was found between the hydrogel and PLC–HA scaffold. Freshly harvested constructs showed apparent tissue ingrowth into microchannels in the distal end of the scaffolds (Fig. 3A–C). Microscopically, isolated areas of vascularization were found in microchannels without any human cells but infiltrated with host cells (Fig. 3D, G) throughout the scaffold. In contrast, substantial vascularization was present in microchannels of the representative scaffold seeded with hMSCs (Fig. 3E, H). Modest vascularization was present in the scaffolds' microchannels seeded with hMSC-derived osteogenic cells (Fig. 3F, I), somewhat similar to the scaffold without any human cells (Fig. 3D, G). Quantitatively, hMSC-seeded scaffolds contained not only significantly more blood vessels, but also blood vessels of significantly larger diameter

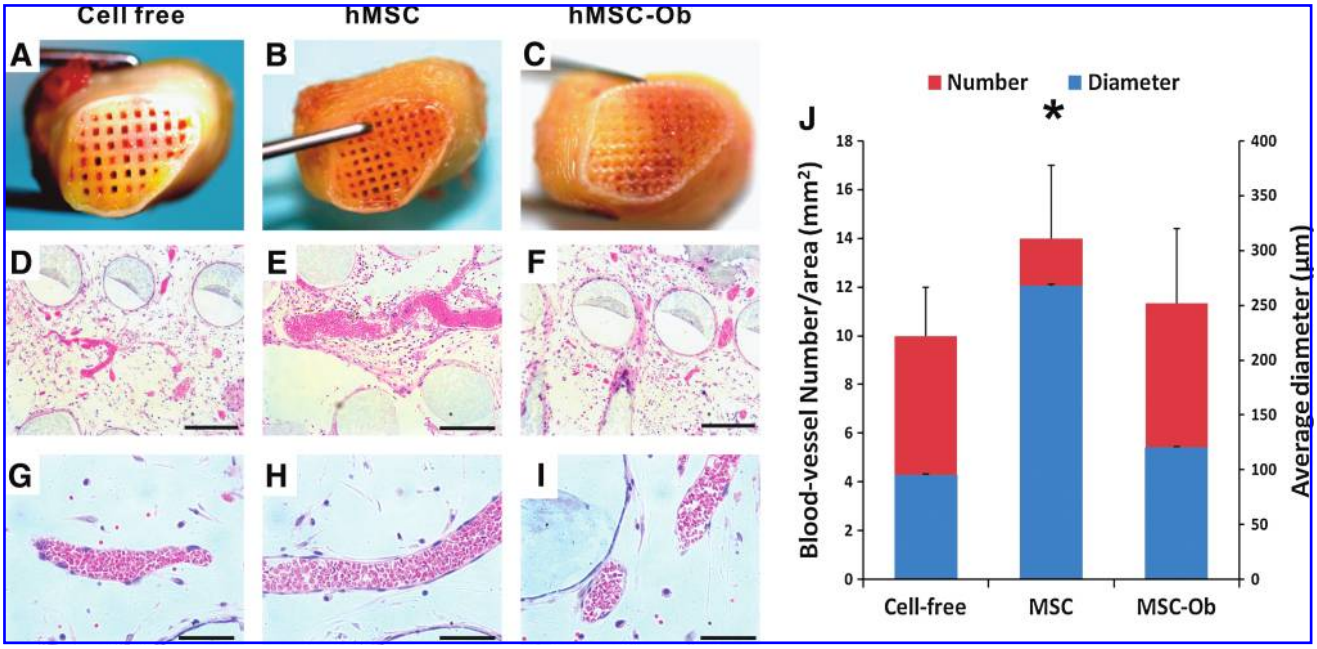

FIG. 3. Angiogenesis in microchannels of *in vivo* harvested synovial joint condyle graft. Gross images of distal ends of *in vivo* retrieved condyle grafts revealed apparent tissue ingrowth into the scaffolds' microchannels seeded without human cells (**A**), hMSCs (**B**) and hMSC-derived osteogenic cells (hMSC-Ob) (**C**). Hematoxylin and eosin–stained microscopic sections showed pronounced vascularization in a MSC-seeded graft (**E, H**) in comparison with modest vascularization in grafts seeded with MSC-derived osteoblasts (**F, I**) or without delivered cells (cell-free) (**D, G**), which nonetheless was populated by host-derived cells. Quantitatively, grafts seeded with MSCs showed not only significantly more blood vessels, but also vessels with significantly greater diameter than MSC-Ob or cell-free samples (**J**) ($n = 10$; $p < 0.05$). There was no significant difference in vascularization between MSC-Ob and cell-free samples ($n = 10$; $p > 0.05$) (**G**). Scale of **D, E, F:** 400 μm, **G, H, I:** 200 μm. *, $p > 0.05$. Color images available online at www.liebertonline.com/ten.

than scaffolds seeded without human cells or seeded with hMSC-derived osteogenic cells ($n = 10$; $p < 0.001$) (Fig. 3J). There were no significant differences in vascular number and diameter of scaffolds seeded without human cells or seeded with hMSC-derived osteoblasts ($n = 10$, $p > 0.05$). No significant differences of tissue genesis and vascularization were found in histomorphometry between distal, middle, and proximal regions.

Formation of mineralized tissue by hMSC-derived osteoblasts

After 6 weeks *in vivo* implantation, von Kossa staining identified little mineralization in cell-free scaffolds, although host cell infiltration was again evident (Fig. 4A). Despite substantial tissue formation in hMSC-seeded scaffolds, little mineralization was found with von Kossa staining (Fig. 4B). In contrast, von Kossa–positive mineralization accumulated on the surface of the scaffolds' microchannels seeded with hMSC-derived osteogenic cells (Fig. 4C). Osteopontin was immunolocalized on the wall of the scaffolds' microchannels seeded with hMSC-derived osteoblasts (Fig. 4D), similar to the distribution of von Kossa–positive mineral deposition in Figure 4C. No positive osteopontin was identified in cell-free scaffolds or hMSC seeded scaffolds (data not shown). Quantitatively, mineralized tissue volume per total tissue volume in scaffolds seeded with hMSC-derived osteogenic cells was in the range of 11.5% to 19.6% (Fig. 4E). No significant difference in mineralization was found between the distal, middle, and proximal regions of the scaffold.

Formation of chondrogenic tissue by hMSC-derived chondrocytes

After 6 weeks of *in vivo* implantation, no host cell or tissue ingrowth was found in cell-free PEGDA hydrogel (Fig. 4F), consistent with our previous findings.[8,15,17–19,21] Abundant cells were present in PEGDA hydrogel encapsulating hMSCs (without chondrogenic differentiation), although safranin O staining revealed little chondrogenesis (Fig. 4G). In contrast, hMSC-derived chondrogenic cells seeded in PEGDA hydrogel yielded safranin O–positive tissue (arrows in Fig. 4H). However, tissue inferior to safranin O–positive cells in scaffolds' microchannels lacked safranin O staining (lower portion of Fig. 4H), suggesting that hMSC-derived osteoblasts seeded inferiorly in microchannels or host cells that had migrated into microchannels may have prevented gel-encapsulated hMSC-derived chondrocytes within the scaffolds' microchannels from undergoing chondrogenesis. Nonetheless, safranin O–positive and –negative tissues were well integrated (Fig. 4H). After 6 weeks of *in vivo* implantation, type II collagen was immunolocalized to the pericellular matrix of hMSC-derived chondrocytes in the PEG hydrogel layer of the osteochondral scaffold (Fig. 4I). No positive type II collagen was identified in cell-free PEGDA hydrogel or hMSC-seeded PEGDA hydrogel (data not shown). There were significantly more cells in the PEGDA hydrogel encapsulating hMSCs than hMSC-derived chondrogenic cells after 6 weeks of *in vivo* implantation ($n = 10$; $p < 0.01$) (Fig. 4J), suggesting that hMSCs proliferated in PEGDA hydrogel *in vivo* or that perhaps hMSC-derived chondrogenic cells proliferated less.

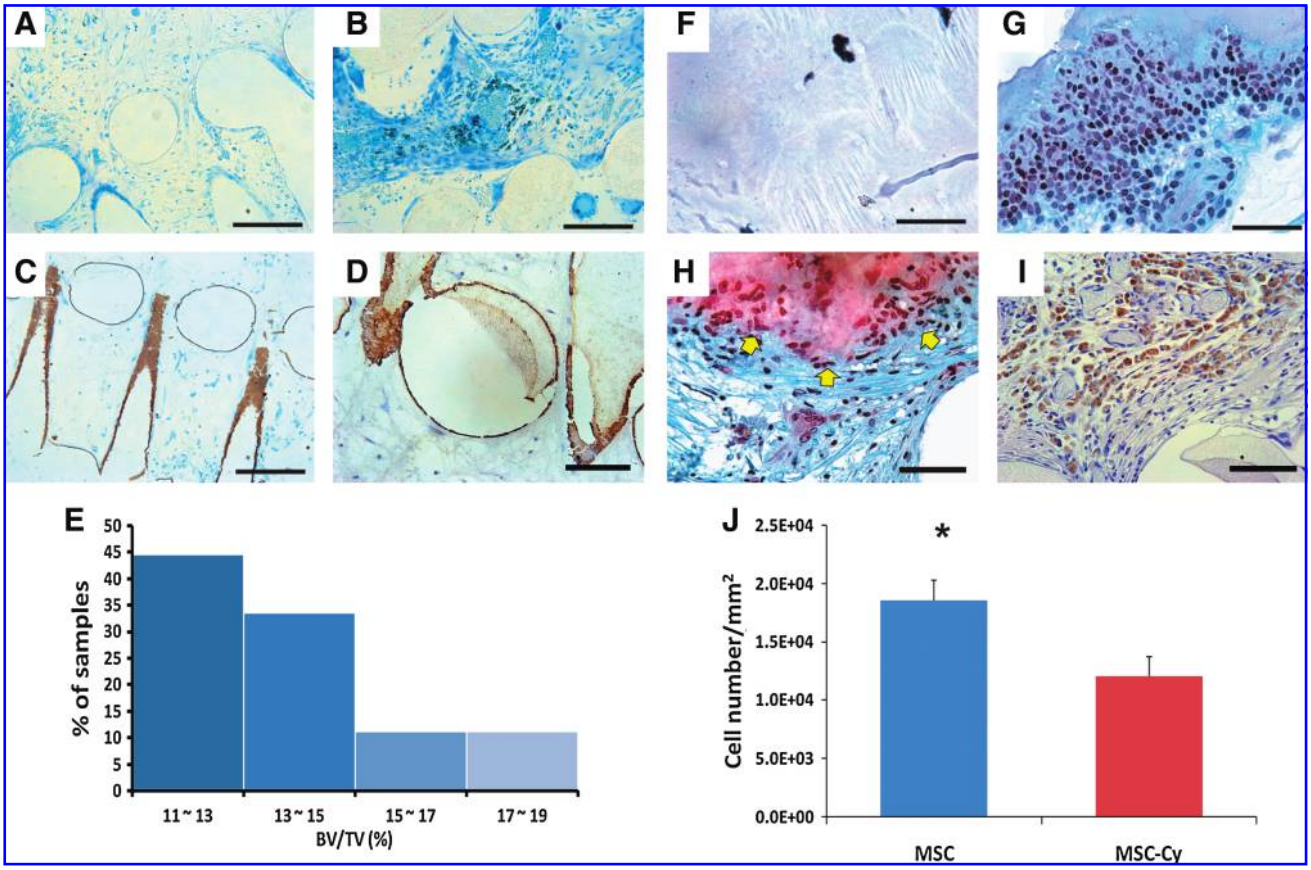

FIG. 4. Histomorphometric and immunohistochemical analyses of bioengineered synovial joint condyle grafts seeded without delivered human cells, with hMSCs, or with hMSC-derived osteogenic cells. After 6 weeks of *in vivo* implantation, von Kossa staining revealed mineralized tissue accumulation on the wall of the scaffolds' microchannels seeded with MSC-Ob (**C**), in comparison with little mineralization of the graft seeded with no delivered human cells (**A**) or hMSCs (**B**). Osteopontin, a late-stage osteogenesis marker, was immunolocalized on the surface of the microchannel wall of the representative graft seeded with hMSC-Ob (**D**), corresponding to von Kossa–positive mineral deposition in **C.** No positive osteopontin was identified with the cell-free PCL-HA scaffold or the hMSC-seeded PCL-HA scaffold (data not shown). Quantitatively, bone volume per total volume in MSC-Ob–seeded grafts was in the range of 11.5% to 19.6% per image analysis of von Kossa–stained sections (**I**) ($n = 10$). Safranin O, a cationic dye staining glycosaminoglycans, was positive in the intercellular matrix of the representative graft seeded with MSC-derived chondrocytes (hMSC-Cy) (**G**), in comparison with little safranin O–positive staining in representative grafts seeded with no delivered human cells (but nonetheless infiltrated by host cells) (**E**) or the representative graft seeded with hMSCs (**F**). Type II collagen was immunolocalized to hMSC-derived chondrocytes encapsulated in hydrogel (**H**). Quantitatively, significantly more cells were present in the hMSC-seeded hydrogel layer than hMSC-Cy (**J**), suggesting that MSCs are more proliferative than MSC-derived chondrocytes because the initial cell density was equal in both groups. Scale: 400 μm (**A–C, F–G**), 200 μm (**D, H, I**). *, $p < 0.01$. Color images available online at www.liebertonline.com/ten.

Discussion

The present scale-up of the human-shaped tibial joint condyle grafts at $20 \times 15 \times 15\,mm^3$ or approximately 25% of the proximal human tibial condyle doubles the size of our previous human-shaped temporomandibular condyle grafts.[8] Modularizing large scaffolds with 400-μm repeats of microchannels enables scale-up because vascularization is required for nutrient diffusion and waste removal over a volume of 200 to 400 μm.[26,27] Microfabrication approaches have recently been adopted to yield internal scaffold structures that accommodate cell seeding, although scale-up of some of the microfabricated scaffolds and *in vivo* performance remain to be tested.[30–32] The present approach of rapid prototyping appears to be effective in generating repeating modulus of 400-μm microchannels that serve as conduits for vascularization and surfaces for cell seeding. We recently fabricated hydrogels with internalized microchannels for soft tissue applications and discovered that microchannels serve as conduits for host-derived vascularization,[33,34] similar to the present microchannel conduits in hard tissue scaffolds. The presently observed cell attachment to the wall of microchannels confirms the utility of the microchanneled scaffold. Not only seeded human cells, but also migration and recruitment of host-derived cells contribute to tissue genesis in the scaffolds' microchannels. To better understand the source of host-derived cells, we are in the process of using several cell-tracking probes, including our recently reported

bioconjugated quantum dots labeling MSCs and progenies,[5] to delineate the fate of delivered cells and the relative contribution of transplanted and host cells in regenerating tissue.

Angiogenesis is an important enabling factor for scale-up. The observed angiogenesis in microchannels after 6 weeks of *in vivo* implantation provides important clues that a probable combination of delivered human cells and host (rat) cells have co-populated the scaffolds' microchannels and anastomized into vasculature. Blood vessels are not only more numerous, but also of greater diameter upon the seeding of hMSCs than hMSC-derived osteoblasts or cell-free scaffolds, suggesting that hMSCs, without differentiation, have the capacity to elaborate angiogenesis and, conversely, that hMSC progenies, such as hMSC-derived osteoblasts, are not as capable of elaborating angiogenesis. Previous reports that MSC-elaborated bioactive molecules increase the synthesis of vascular endothelial growth factor and vascular density confirm this.[36,37] In the present study, not only modular scaffolds with repeat units of internal microchannels, but also hMSCs that elaborated angiogenesis, improved tissue formation and vascularization.

Cell number in the bioengineered cartilage portion is significantly greater upon seeding of hMSCs than hMSC-derived chondrocytes. No angiogenesis is present in the hydrogel layer that incorporates MSCs or MSC-derived chondrocytes. What prevents angiogenesis in bioengineered cartilage seeded with MSCs or MSC-derived chondrocytes? An interesting observation of the present work is that hMSC-derived chondrogenic cells seeded in PEGDA hydrogel yield safranin O–positive tissue reminiscent of the matrix of native chondrocytes. However, tissue inferior to safranin O–positive cells in the scaffolds' microchannels seeded with hMSC-derived chondrocytes lacks safranin O staining, suggesting that hMSC-derived osteoblasts seeded inferiorly in microchannels or host cells that have migrated into microchannels prevent gel-encapsulated hMSC-derived chondrocytes within the scaffolds' microchannels from undergoing angiogenesis. The prevention of angiogenesis in articular cartilage has received little attention from the tissue engineering community but is probably an important matter that warrants additional studies.

Layer-fabricated scaffolds with repeating units of microchannels represent another step toward functional synovial joint regeneration *in situ* by enabling scale-up of a tissue engineering construct. This is a further extension of our previous work[31,32] using porous scaffolds fabricated with a different rapid prototyping approach and different materials (PCL in previous studies vs PCL–HA in the present study). Compared with a recent study of a scale-up construct seeded with chondrocytes in the smallest dimension of 5 mm,[24] tissue genesis was remarkable in the present study with the smallest scaffold dimension of 15 mm. An important advantage of microchanneled scaffolds for synovial joint regeneration is a balance between their mechanical stiffness similar to bone[38,39] and accommodation of cell seeding and angiogenesis in the scaffolds' microchannels. The present data regarding tissue formation and vascularization in by far one of the largest synovial joint condyle grafts *in vivo* suggest that scale-up is possible by conduits of microchannels that accommodate and enable host-derived angiogenesis and by MSCs.

Acknowledgments

We thank Sarah Kennedy and Fen Guo for administrative and technical assistant. This work was supported by National Institutes of Health grant EB02332 to J.J.M.

Author Disclosure Statement

No competing financial interests exist.

References

1. National and State Medical Expenditures and Lost Earnings Attributable to Arthritis and Other Rheumatic Conditions—United States, 2003 [on-line]. Available at www.cdc.gov/mmwr/preview/mmwrhtml/mm5601a2.htm Accessed October 15, 2008.
2. Archer, C.W., Dowthwaite, G.P., Francis-West, P. Development of synovial joints. Birth Defects Res C Embryo Today **69,** 144, 2003.
3. Hunziker, E.B. Growth-factor-induced healing of partial-thickness defects in adult articular cartilage. Osteoarthritis Cartilage **9,** 22, 2001.
4. Leddy, H.A., Guilak, F. Site-specific effects of compression on macromolecular diffusion in articular cartilage. Biophys J **95,** 4890, 2008.
5. Pacifici, M., Koyama, E., Iwamoto, M., Gentili, C. Development of articular cartilage: what do we know about it and how may it occur? Connect Tissue Res **41,** 175, 2000.
6. Shieh, A.C., Athanasiou, K.A. Principles of cell mechanics for cartilage tissue engineering. Ann Biomed Eng **31,** 1, 2003.
7. Volk, S.W., Leboy, P.S. Regulating the regulators of chondrocyte hypertrophy. J Bone Miner Res **14,** 483, 1999.
8. Alhadlaq, A., Mao, J.J. Tissue-engineered osteochondral constructs in the shape of an articular condyle. J Bone Joint Surg Am **87,** 936, 2005.
9. Elisseeff, J., Puleo, C., Yang, F., Sharma, B. Advances in skeletal tissue engineering with hydrogels. Orthod Craniofac Res **8,** 150, 2005.
10. Oxley, H.R., Corkhill, P.H., Fitton, J.H., Tighe, B.J. Macroporous hydrogels for biomedical applications: methodology and morphology. Biomaterials **14,** 1064, 1993.
11. Peppas, N.A., Huang, Y., Torres-Lugo, M., Ward, J.H., Zhang, J. Physicochemical foundations and structural design of hydrogels in medicine and biology. Annu Rev Biomed Eng **2,** 9, 2000.
12. Mao, J.J. Stem-cell-driven regeneration of synovial joints. Biol Cell **97,** 289, 2005.
13. Buckwalter, J.A., Martin, J.A. Osteoarthritis. Adv Drug Deliv Rev **58,** 150, 2006.
14. Goldberg, V.M., Caplan, A.I. Biological resurfacing: an alternative to total joint arthroplasty. Orthopedics **17,** 819, 1994.
15. Grayson, W.L., Chao, P.H., Marolt, D., Kaplan, D.L., Vunjak-Novakovic, G. Engineering custom-designed osteochondral tissue grafts. Trends Biotechnol **26,** 181, 2008.
16. Tuan, R.S. A second-generation autologous chondrocyte implantation approach to the treatment of focal articular cartilage defects. Arthritis Res Ther **9,** 109, 2007.
17. Alhadlaq, A., Elisseeff, J.H., Hong, L., Williams, C.G., Caplan, A.I., Sharma, B., Kopher, R.A., Tomkoria, S., Lennon, D.P., Lopez, A., Mao, J.J. Adult stem cell driven genesis of human-shaped articular condyle. Ann Biomed Eng **32,** 911, 2004.
18. Martin, I., Miot, S., Barbero, A., Jakob, M., Wendt, D. Osteochondral tissue engineering. J Biomech **40,** 750, 2007.

19. Troken, A., Marion, N., Hollister, S., Mao, J. Tissue engineering of the synovial joint: the role of cell density. Proc Inst Mech Eng [H] **221,** 429, 2007.
20. Wang, L., Detamore, M.S. Tissue engineering the mandibular condyle. Tissue Eng **13,** 1955, 2007.
21. Weng, Y., Cao, Y., Silva, C.A., Vacanti, M.P., Vacanti, C.A. Tissue-engineered composites of bone and cartilage for mandible condylar reconstruction. J Oral Maxillofac Surg **59,** 185, 2001.
22. Vunjak-Novakovic, G., Meinel, L., Altman, G., Kaplan, D. Bioreactor cultivation of osteochondral grafts. Orthod Craniofac Res **8,** 209, 2005.
23. Isogai, N., Landis, W., Kim, T.H., Gerstenfeld, L.C., Upton, J., Vacanti, J.P. Formation of phalanges and small joints by tissue-engineering. J Bone Joint Surg Am **81,** 306, 1999.
24. Hoang, N.T., Hoehnke, C., Hien, P.T., Mandlik, V., Feucht, A., Staudenmaier, R. Neovascularization and free microsurgical transfer of in vitro cartilage-engineered constructs. Microsurgery **29,** 52, 2009.
25. Moutos, F.T., Freed, L.E., Guilak, F. A biomimetic three-dimensional woven composite scaffold for functional tissue engineering of cartilage. Nat Mater **6,** 162, 2007.
26. Jain, R.K., Au, P., Tam, J., Duda, D.G., Fukumura, D. Engineering vascularized tissue. Nat Biotechnol **23,** 821, 2005.
27. Muschler, G.F., Nakamoto, C., Griffith, L.G. Engineering principles of clinical cell-based tissue engineering. J Bone Joint Surg Am **86-A,** 1541, 2004.
28. Marion, N.W., Mao, J.J. Mesenchymal stem cells and tissue engineering. Methods Enzymol **420,** 339, 2006.
29. Sundaramurthy, S., Mao, J.J. Modulation of endochondral development of the distal femoral condyle by mechanical loading. J Orthop Res **24,** 229, 2006.
30. Gillette, B.M., Jensen, J.A., Tang, B., Yang, G.J., Bazargan-Lari, A., Zhong, M., Sia, S.K. In situ collagen assembly for integrating microfabricated three-dimensional cell-seeded matrices. Nat Mater **7,** 636, 2008.
31. Schek, H.T. 3rd, Hunt, A.J. Micropatterned structures for studying the mechanics of biological polymers. Biomed Microdevices **7,** 41, 2005.
32. Schek, R.M., Taboas, J.M., Segvich, S.J., Hollister, S.J., Krebsbach, P.H. Engineered osteochondral grafts using biphasic composite solid free-form fabricated scaffolds. Tissue Eng **10,** 1376, 2004.
33. Stosich, M.S., Bastian, B., Marion, N.W., Clark, P.A., Reilly, G., Mao, J.J. Vascularized adipose tissue grafts from human mesenchymal stem cells with bioactive cues and microchannel conduits. Tissue Eng **13,** 2881, 2007.
34. Stosich, M.S., Moioli, E.K., Wu, J.K., Lee, C.H., Rohde, C., Yoursef, Z.M., Ascherman, J., Diraddo, R., Marion, M.W., Mao, J.J. Bioengineering strategies to generate vascularized soft tissue grafts with sustained shape. Methods **47,** 116, 2009.
35. Shah, B.S., Clark, P.A., Moioli, E.K., Stroscio, M.A., Mao, J.J. Labeling of mesenchymal stem cells by bioconjugated quantum dots. Nano Lett **7,** 3071, 2007.
36. Caplan, A.I., Dennis, J.E. Mesenchymal stem cells as trophic mediators. J Cell Biochem **98,** 1076, 2006.
37. Tang, Y.L., Zhao, Q., Zhang, Y.C., Cheng, L., Liu, M., Shi, J., Yang, Y.Z., Pan, C., Ge, J., Phillips, M.I. Autologous mesenchymal stem cell transplantation induce VEGF and neovascularization in ischemic myocardium. Regul Pept **117,** 3, 2004.
38. Ang, K.C., Leong, K.F., Chua, C.K., Chandrasekaran, M. Compressive properties and degradability of poly(epsilon-caprolactone)/hydroxyapatite composites under accelerated hydrolytic degradation. J Biomed Mater Res A **80,** 655, 2007.
39. Williams, J.M., Adewunmi, A., Schek, R.M., Flanagan, C.L., Krebsbach, P.H., Feinberg, S.E., Hollister, S.J., Das, S. Bone tissue engineering using polycaprolactone scaffolds fabricated via selective laser sintering. Biomaterials **26,** 4817, 2005.

Address correspondence to:
Jeremy J. Mao, D.D.S., Ph.D.
Columbia University Medical Center
630 W. 168 Street – PH7E – CDM
New York, NY 10032

E-mail: jmao@columbia.edu

Received: October 30, 2008
Accepted: June 29, 2009
Online Publication Date: November 4, 2009

This article has been cited by:

1. BB Ward, SE Brown, PH Krebsbach. 2010. Bioengineering strategies for regeneration of craniofacial bone: a review of emerging technologies. *Oral Diseases* no-no. [CrossRef]